Cell Reports Medicine, Volume *5*

Supplemental information

Thymosin α1 reverses oncolytic adenovirus-induced M2 polarization of macrophages to improve antitumor immunity and therapeutic efficacy

Kua Liu, Lingkai Kong, Huawei Cui, Louqian Zhang, Qilei Xin, Yan Zhuang, Ciliang Guo, Yongzhong Yao, Jinqiu Tao, Xiaosong Gu, Chunping Jiang, and Junhua Wu

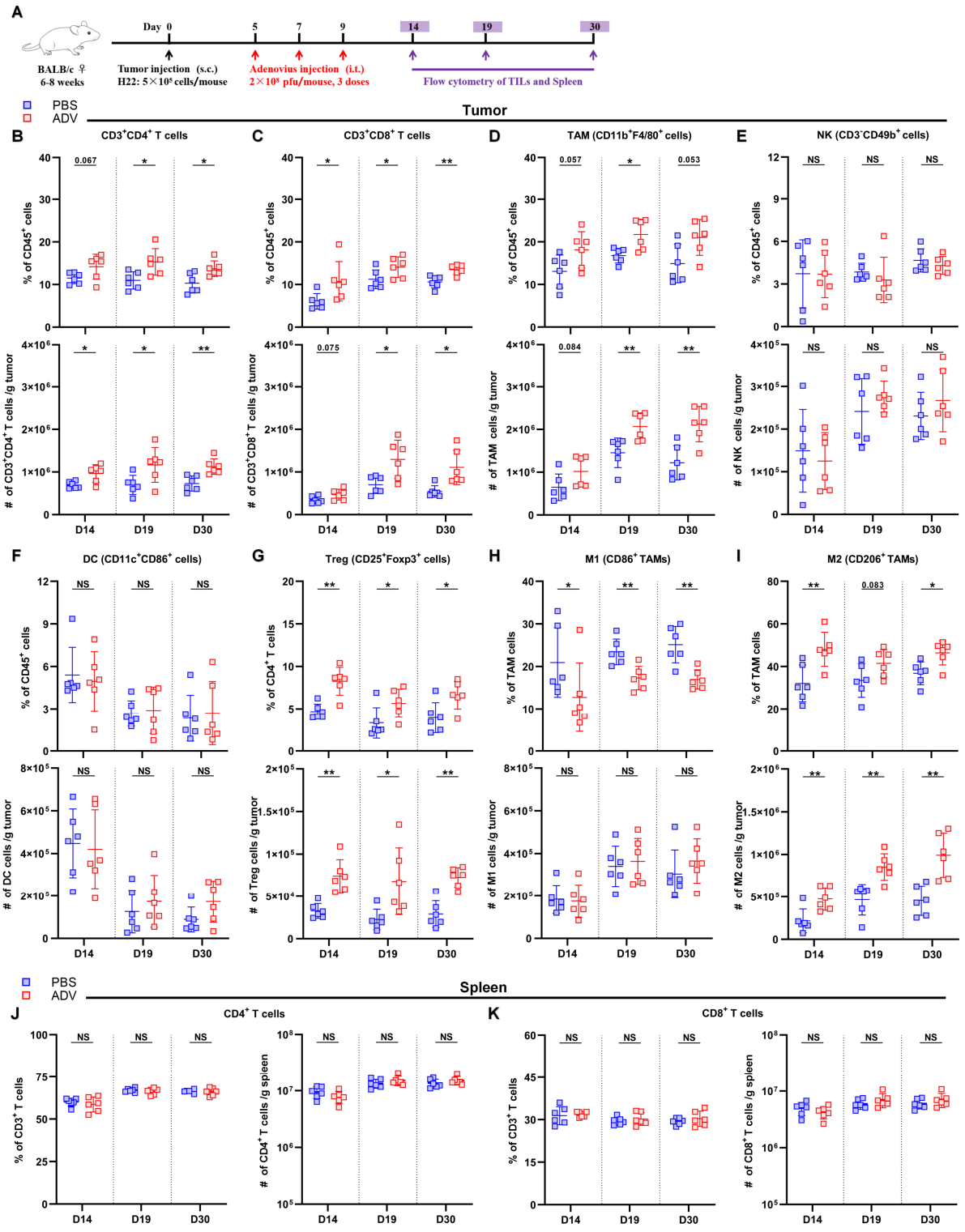

Figure S1. ADV treatment effectively increased tumor immune infiltration while induced an immunosuppressive feedback loop in HCC model. Related to Figure 1.

(A) Experimental schematic of mice from (Figures S1B-S1K): H22-tumor-bearing wild-type (WT) mice were administered ADV or vehicle control (PBS) starting on day 5 when the tumor volume reached approximately 50

to 100 mm^3. Tumor-infiltrating leukocytes (TILs) from the tumor and spleen were assessed by flow cytometry (day 14, day 19, day 30; n=6 biological replicates); s.c., subcutaneous; i.t., intratumoral. **(B-I)** Percentages (top) and total cells normalized to g tumor tissue (bottom) of Tumor-infiltrating **(B)** $CD3^+CD4^+$ T cells, **(C)** $CD3^+CD8^+$ T cells, **(D)** $CD11b^+F4/80^+$ macrophages, **(E)** $CD3^-CD49b^+$ NK cells, **(F)** $CD11c^+CD86^+$ DCs, **(G)** $CD25^+Foxp3^+$ Treg cells, **(H)** "M1-like" macrophages, **(I)** "M2-like" macrophages within the TME of mice (n=6 biological replicates). **(J and K)** Percentages (left) and total cells normalized to g tumor tissue (right) of $CD4^+$ T cells **(J)** and $CD8^+$ T cells **(K)** within the spleens of mice (n=6 biological replicates). The data are shown as the means ± SD. NS, no significant difference; *$p<0.05$, **$p<0.01$.

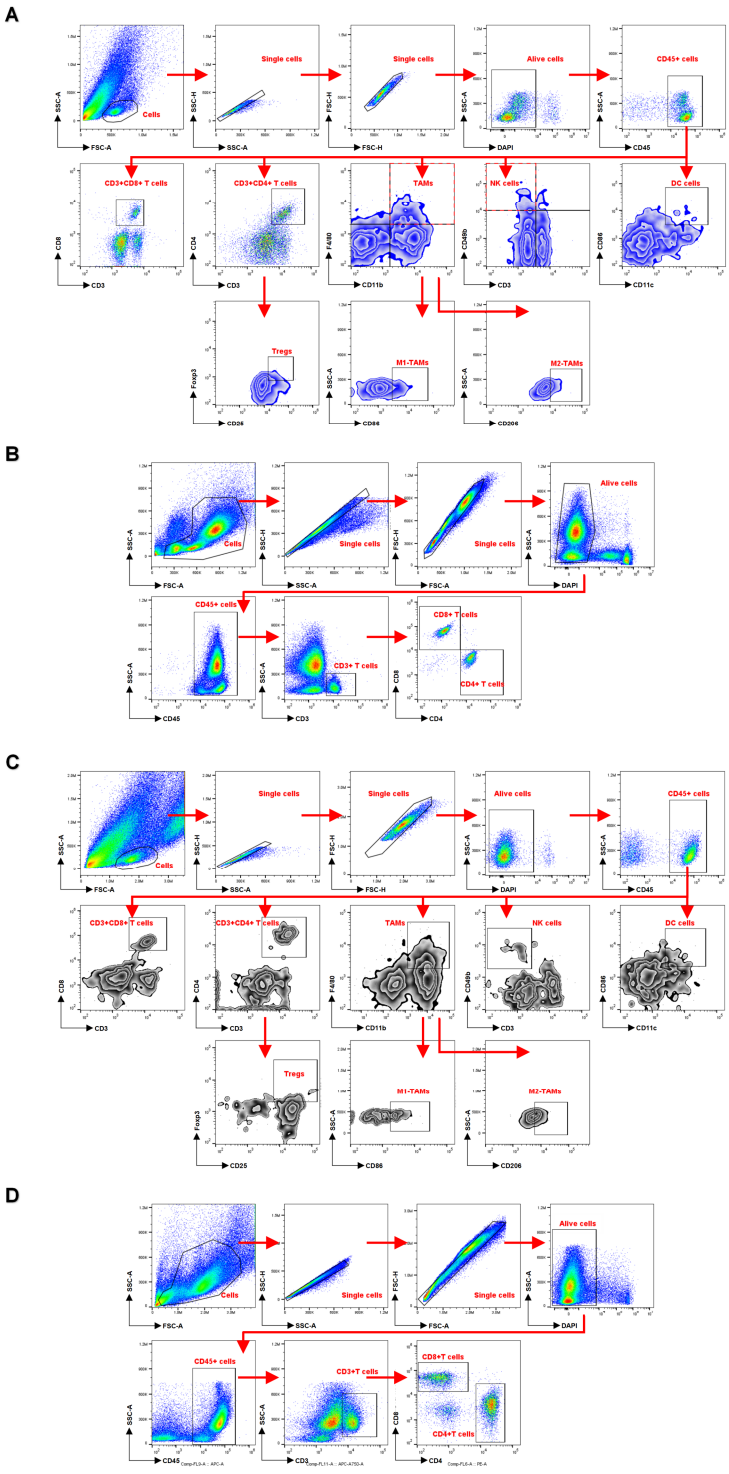

Figure S2. Flow cytometry gating strategy for the identification of immune cells within the tumor and spleen. Related to Figure 1 and Figure S1.

(A) Flow cytometry gating strategy for the identification of immune cells within the tumor in 4T1 model. **(B)** Flow cytometry gating strategy for the identification of immune cells within the spleen in 4T1 model. **(C)** Flow

cytometry gating strategy for the identification of immune cells within the tumor in H22 model. **(D)** Flow cytometry gating strategy for the identification of immune cells within the spleen in H22 model.

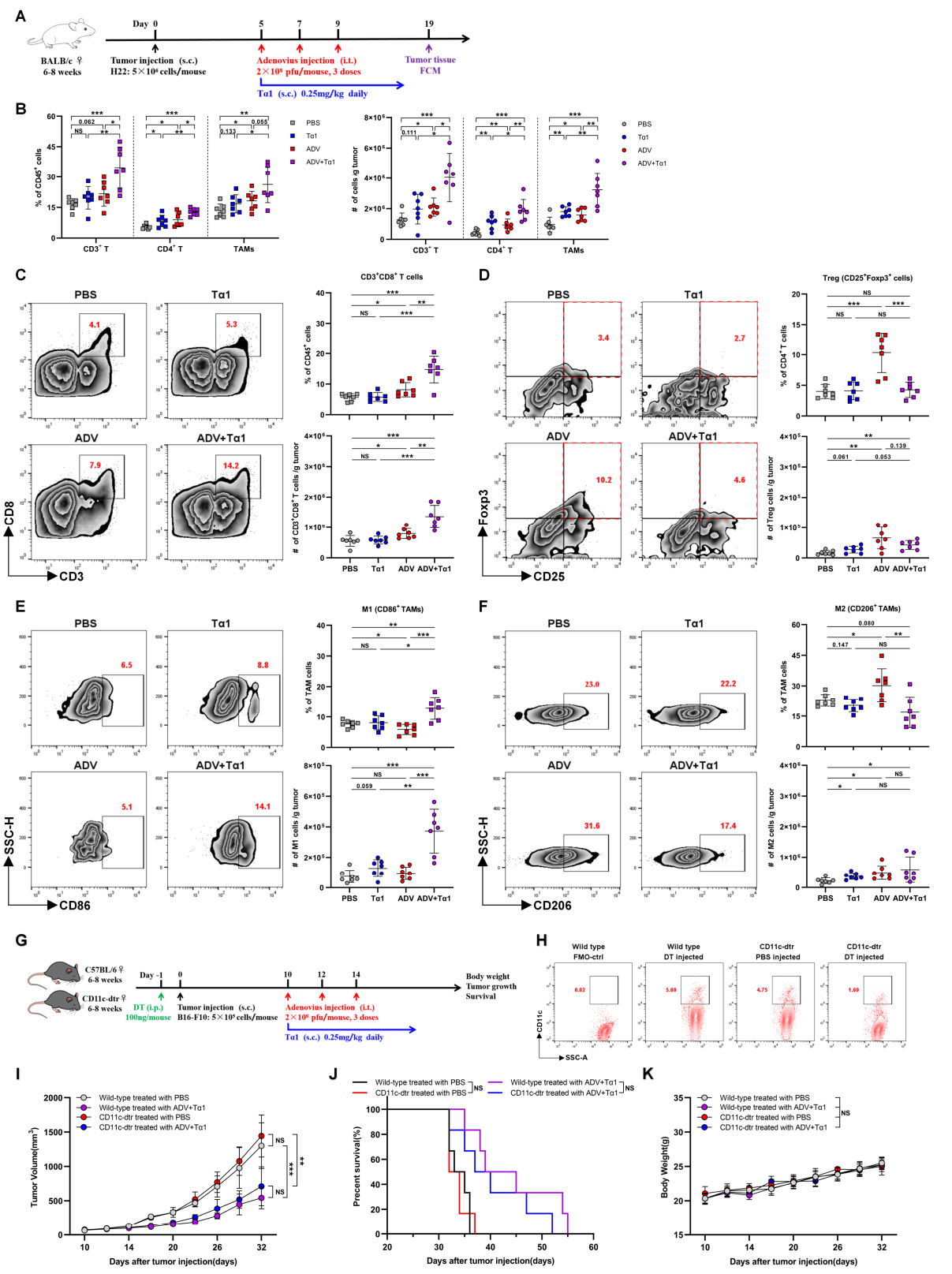

Figure S3. Tα1 intervention can reprogram the TME during ADV treatment. Related to Figure 3.

(A) Schematic representation of experimental design and treatment timeline. Wild-type mice were injected subcutaneously with 5×10^6 H22 cells. When the tumor volume reached approximately 50 to 100 mm^3, the mice

were randomly divided into different groups and treated with an intratumoral injection of 0.1 mL of PBS or ADV (2×10^8 PFUs) every 2 days for a total of three times. Tα1 (0.25 mg/kg) was injected subcutaneously into the peritumoral site once daily starting with the first dose of ADV. Tumor-infiltrating leukocytes (TILs) from the tumor were assessed by flow cytometry (day 19; n=7 biological replicates); s.c., subcutaneous; i.t., intratumoral. **(B)** Percentages (left) and total cells normalized to g tumor tissue (right) of $CD3^+$ T cells, $CD4^+$ T cells and TAMs within the TME of mice (n=6 biological replicates). **(C-F)** Representative plots (left), percentages (top) and total cells normalized to g tumor tissue (bottom) of Tumor-infiltrating **(C)** $CD3^+CD8^+$ T cells, **(D)** $CD25^+Foxp3^+$ Treg cells, **(E)** "M1-like" macrophages and **(F)** "M2-like" macrophages within the TME of mice (n=6 biological replicates). **(G-K)** Wild-type (WT) mice and CD11c-dtr mice were administered diphtheria toxin the day before tumor injection. B16 tumor-bearing mice were administered different immunotherapies starting on day 10 when the tumor volume reached approximately 50 to 100 mm^3 (n=6 biological replicates). s.c., subcutaneous; i.t., intra-tumoral; i.p., intra-peritoneal. **(G)** Schematic representation of experimental design and treatment timeline. **(H)** Tumor tissue samples of B16 tumor-bearing mice were collected on day 10, and flow cytometry confirmed the depletion effect of diphtheria toxin on CD11c-dtr mice. **(I)** Tumor growth. **(J)** Survival. **(K)** Body weight. The data are shown as the means ± SD. NS, no significant difference; *p<0.05, **p<0.01, ***p<0.001.

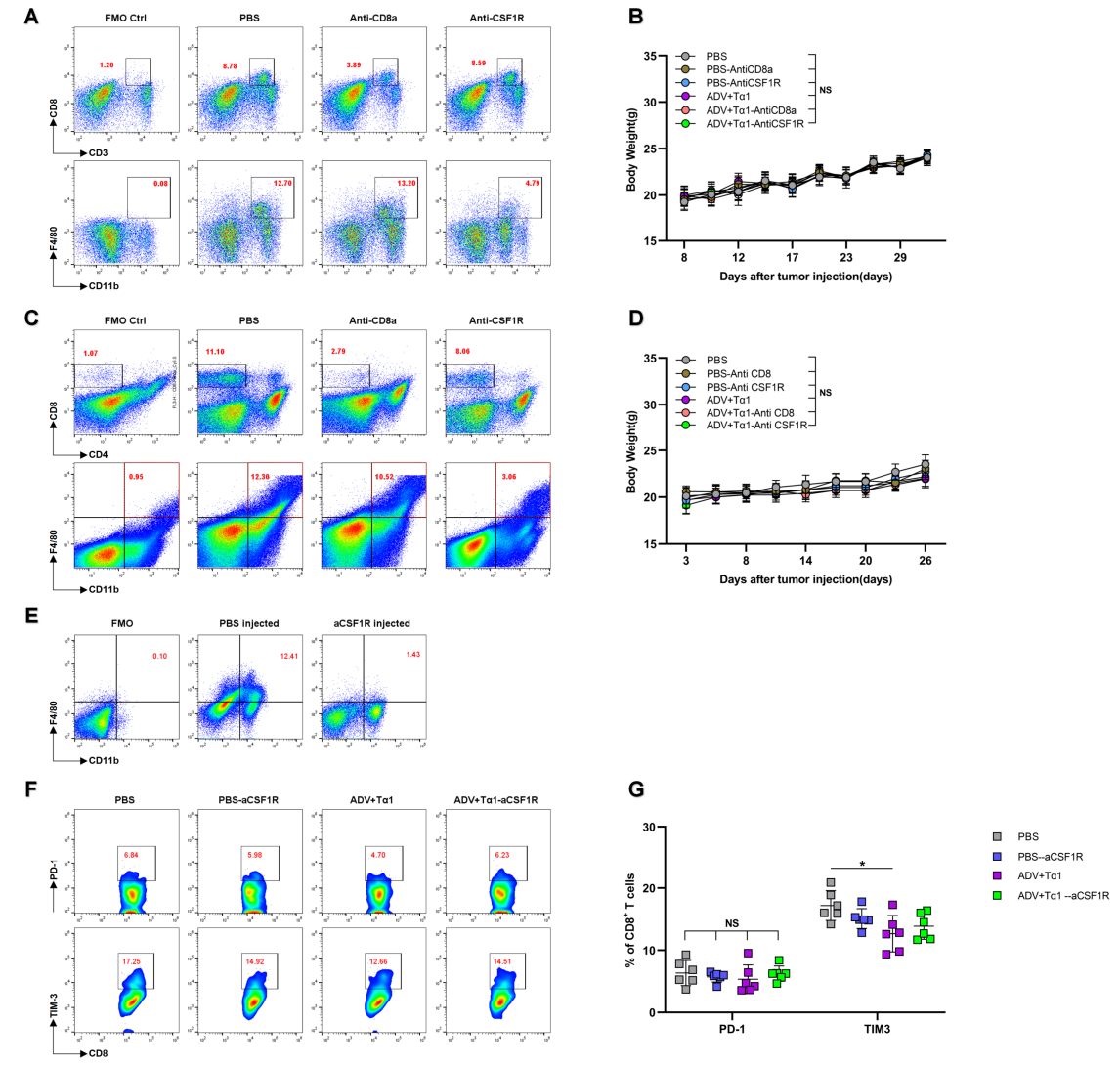

Figure S4. The antitumor activity of ADV combined with Tα1 was mediated by macrophages and CD8$^+$ T cells. Related to Figure 4.

(A) Tumor tissue samples of 4T1 tumor-bearing mice (from Figure 4B) were collected on day 15, and flow cytometry confirmed the anti-CSF1R and anti-CD8a depletion effects. **(B)** Body weight of 4T1 tumor -bearing mice (from Figures 4B and 4C) was monitored every 2 or 3 days (n=10 biological replicates). **(C)** Tumor tissue samples of H22-bearing mice (from Figure 4C) were collected on day 15, and flow cytometry confirmed the anti-CSF1R and anti-CD8a depletion effects. **(D)** Body weight of H22-bearing mice (from Figures 4C and 4D) was monitored every 2 or 3 days in the H22 model (n=10 biological replicates). **(E)** Tumor tissue samples of 4T1-bearing mice (from Figure 4J) were collected on day 15, and flow cytometry confirmed the anti-CSF1R

depletion effect. **(F and G)** Representative plots **(F)** and percentages **(G)** of $PD1^+$ $CD8^+$ T cells and $TIM3^+$ $CD8^+$ T cells within the TME of mice (from Figure 4J; n=6 biological replicates). The data are shown as the means ± SD. NS, no significant difference; *p<0.05.

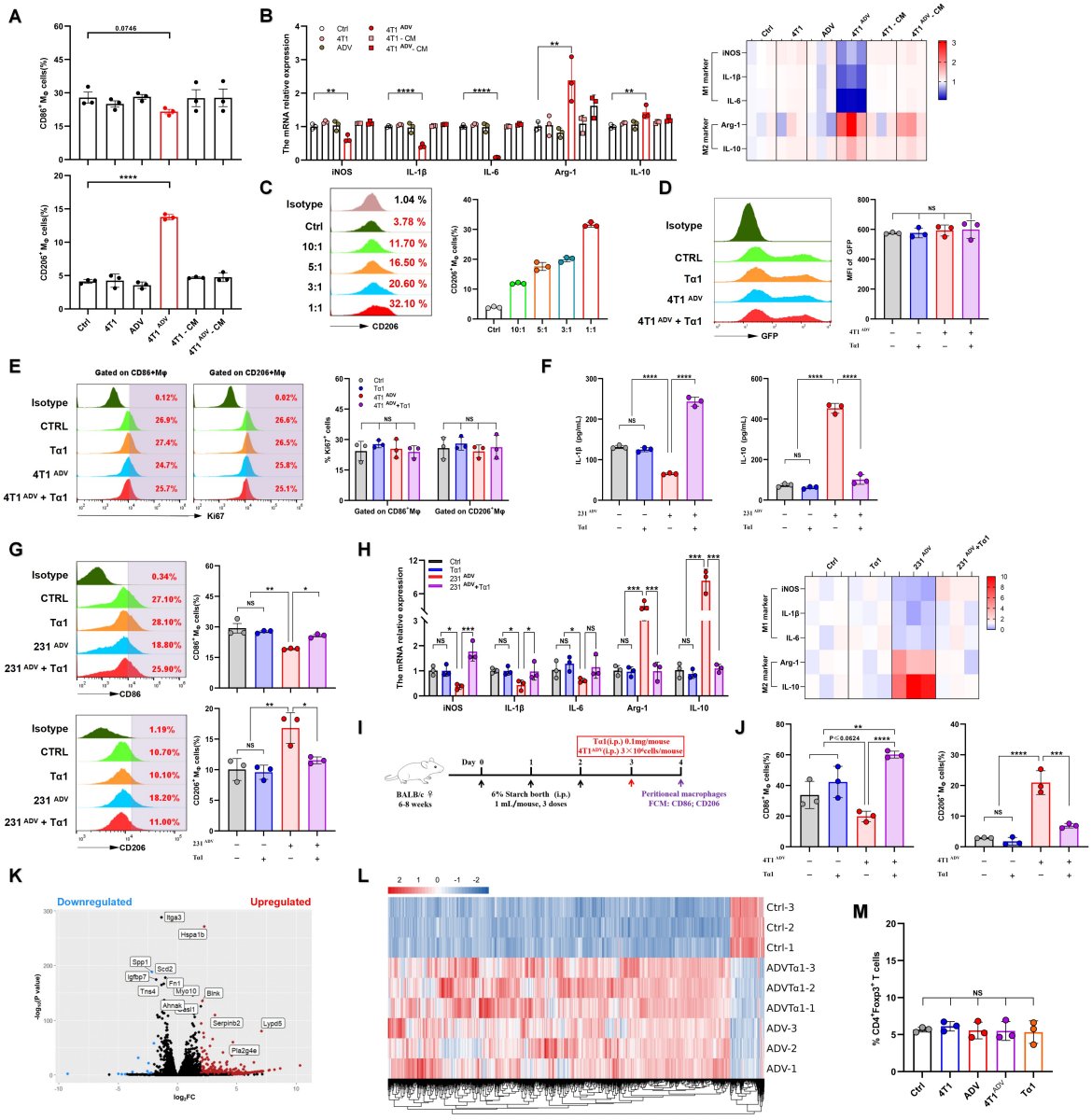

Figure S5. Tα1 reversed the phenotype of macrophages induced by ADV-infected tumor cells. Related to Figure 5.

(A and B) Macrophages (RAW264.7 cells) were cocultured with 4T1 cells, ADV, ADV-infected 4T1 cells (4T1^{ADV} cells), conditioned medium obtained from 4T1 cell cultures (4T1-CM), or 4T1^{ADV}-CM, followed by analysis of macrophage polarization (n=3 biological replicates). **(A)** Expression of CD86 and CD206 was measured by FCM in macrophages. **(B)** Expression of iNOS, IL-1β, IL-6, Arg-1 and IL-10 was measured by qPCR in macrophages (n=3 biological replicates and 3 technical replicates), and the mRNA expression level of

iNOS, IL-1β, IL-6, Arg-1 and IL-10 was showed as heat map. **(C)** Expression of CD206 was measured by FCM in macrophages stimulated by $4T1^{ADV}$ cells at different E:T ratios (n=3 biological replicates). **(D)** After different interventions, macrophages (from Figure 5A) were cocultured with GFP+ *Escherichia coli* for 3 hours. Then, the EGFP levels in macrophages were measured by flow cytometry to assess phagocytosis efficiency. Macrophages from different intervention groups were mixed together to be used as a control to exclude interference from adenovirus GFP fluorescence (n=3 biological replicates). **(E)** Expression of Ki67 was measured by FCM in $CD86^+$ macrophages or $CD206^+$ macrophages (from Figure 5C). **(F-H)** Macrophages (THP-1 cells) were cocultured with stimulated by different interventions, followed by analysis of macrophage polarization (n=3 biological replicates). **(F)** IL-1β and IL-10 concentrations in the supernatants were measured by ELISA. **(G)** The expression of CD86 (top) and CD206 (bottom) in macrophages was measured by FCM. **(H)** The expression of iNOS, IL-1β, IL-6, Arg-1 and IL-10 in macrophages was measured by qPCR, and the mRNA expression levels of iNOS, IL-1β, IL-6, Arg-1 and IL-10 are shown as heatmaps. **(I and J)** BALB/c mice were intraperitoneally injected with 1 mL of 6% starch broth once a day for three days to recruit macrophages. On day 4, PBS, Tα1, $4T1^{ADV}$ cells, or $4T1^{ADV}$ & Tα1 were intraperitoneally injected into mice. On day 5, the mice were euthanized, and the peritoneal macrophages were harvested. **(I)** Schematic representation of experimental design. **(J)** Expression of CD86 and CD206 in peritoneal macrophages was measured by FCM (n=3 biological replicates). i.p., intraperitoneal. **(K)** Volcano plot showing the DEGs between ADV-treated 4T1 cells and vehicle-treated 4T1 cells. DEGs with an absolute log-transformed fold change >1 and a P value <0.05 (determined by two-sided Wilcoxon rank-sum test) were defined as significant. **(L)** Heatmap of DEGs in all 4T1 cell groups. **(M)** $CD4^+$ T cells from mouse spleens were cocultured with 4T1 cells, ADV, or ADV-infected 4T1 cells ($4T1^{ADV}$ cells) or stimulated with Tα1. The expression of Foxp3 in $CD4^+$ T cells was measured by FCM (n=3 biological replicates). The data are shown as the means ± SD. ns, no significant difference; *p<0.05,

**p<0.01, ***p<0.001, ****p<0.0001.

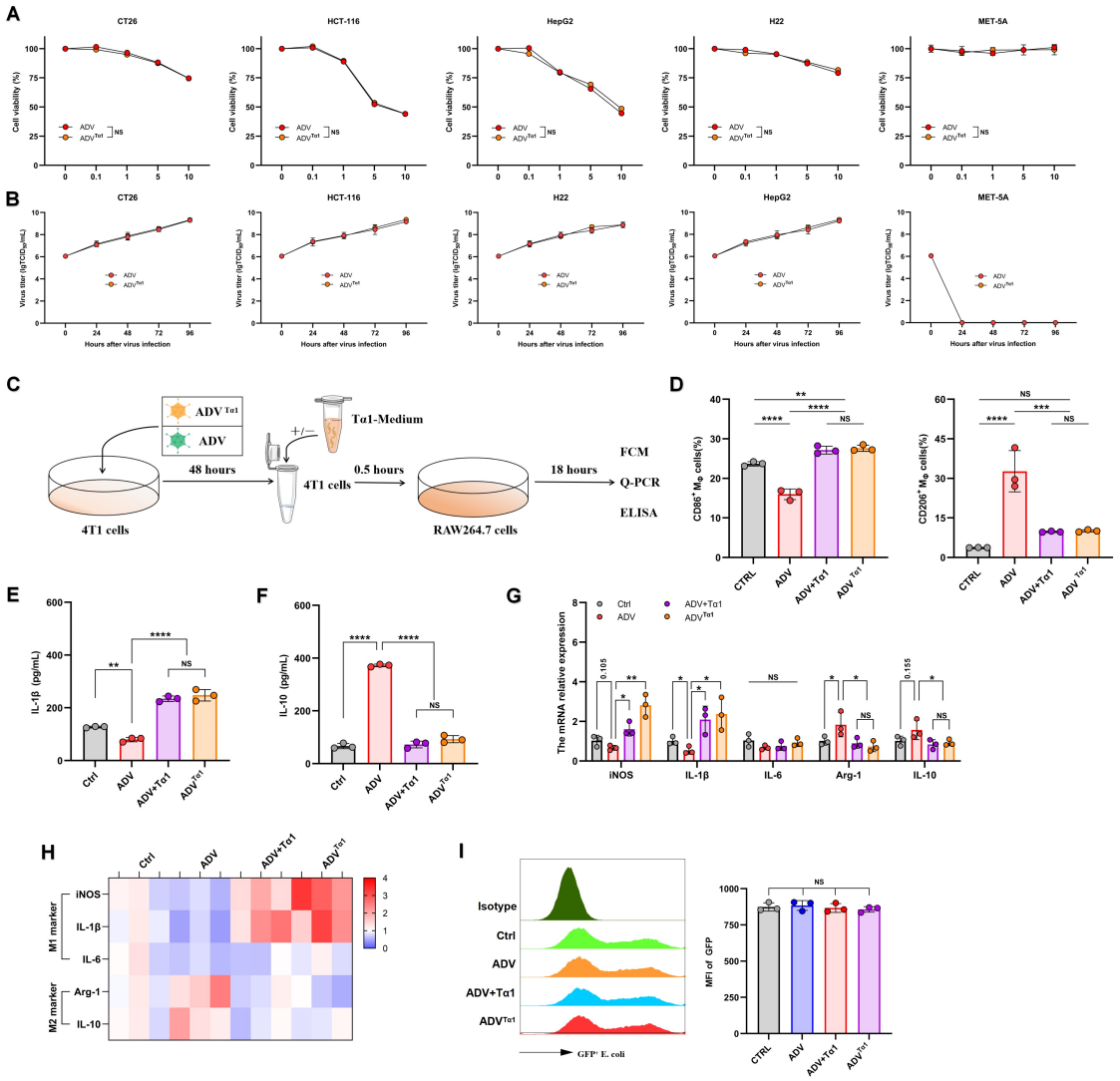

Figure S6. ADV^{Tα1} has replication and oncolytic efficacy similar to that of ADV. Related to Figure 6.

(A) CT26 cells, HCT116 cells, HepG2 cells, H22 cells and MET-5A cells were infected with ADV^{Tα1} or ADV at different MOIs, and cell viability was measured 48 h later by CCK-8 assay (n=3 biological replicates). **(B)** CT26 cells, HCT116 cells, HepG2 cells, H22 cells and MET-5A cells were infected with ADV^{Tα1} or ADV at an MOI of 1. The virus titers were measured by TCID50 assay at different time points after infection (n=3 biological replicates). **(C-H)** Macrophages (RAW264.7 cells) were cocultured with 4T1^{ADV} (ADV), 4T1^{ADV} cells with Tα1 (ADV + Tα1), or ADV^{Tα1}-infected 4T1 cells (ADV^{Tα1}), followed by analysis of macrophage polarization (n=3 biological replicates). **(C)** Schematic representation of experimental design. **(D)** The expression of CD86 (left) and CD206 (right) in macrophages was measured by FCM. **(E)** IL-1β and **(F)** IL-10 (right) concentrations in the

supernatants were measured by ELISA. **(G)** The expression of iNOS, IL-1β, IL-6, Arg-1 and IL-10 in macrophages was measured by qPCR (n=3 biological replicates and 3 technical replicates). **(H)** The mRNA expression levels of iNOS, IL-1β, IL-6, Arg-1 and IL-10 (Figure S6G) are shown as heatmaps. **(I)** After different interventions, macrophages (from Figure 6G) were cocultured with GFP+ *Escherichia coli* for 3 hours. Then, the EGFP levels in the macrophages were measured by flow cytometry to assess the phagocytosis efficiency. Macrophages from different intervention groups were mixed together to be used as a control to exclude interference from adenovirus GFP fluorescence (n=3 biological replicates). The data are shown as the means ± SD. NS, no significant difference; *p<0.05, **p<0.01, ***p<0.001, ****p<0.0001.

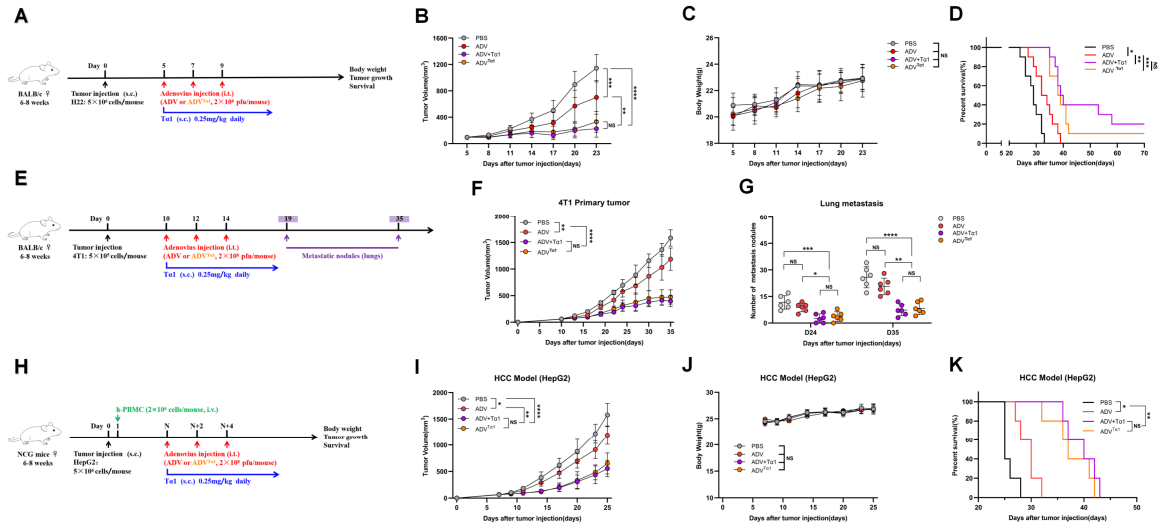

Figure S7. ADV$^{T\alpha1}$ is superior to ADV in producing a better antitumor immune response. Related to Figure 7.

(A-D) H22-tumor-bearing wild-type (WT) mice were administered different immunotherapies or vehicle control (PBS) starting on day 5 when the tumor volume reached approximately 50 to 100 mm^3; s.c., subcutaneous; i.t., intra-tumoral. **(A)** Schematic representation of experimental design and treatment timeline. **(B)** Tumor growth. **(C)** Body weight. **(D)** Survival (n=10 biological replicates). **(E-G)** 4T1 cells were injected into the fourth mammary fat pads of NCG mice, and these 4T1-bearing mice were administered different immunotherapies starting on day 10; s.c., subcutaneous; i.t., intratumoral. **(E)** Schematic representation of experimental design and treatment timeline. Primary tumor growth **(F)** and metastasis to the lung **(G)** in 4T1 tumor -bearing mice after immunotherapies (day 19, 24; n=6 biological replicates). **(H-K)** Tumor-bearing NCG mice were intravenously injected with human peripheral blood mononuclear cells on day 1, and then PBMC-humanized mice were administered different immunotherapies; s.c., subcutaneous; i.t., intra-tumoral; i.v., intravenous. **(H)** Schematic representation of experimental design and treatment timeline. **(I)** Tumor growth. **(J)** Body weight. **(K)** Survival (n=5 biological replicates). The data are shown as the means ± SD. NS, no significant difference; *p<0.05, **p<0.01, ***p<0.001, ****p<0.0001.

Target Name	Forward primer (5' → 3')	Reverse primer (5' → 3')
mArg-1	CAGATATGCAGGGAGTCACC	CAGAAGAATGGAAGAGTCAG
miNOS	CCACCCGAGCTCCTGGAAC	CCCTCCTGATCTTGTGTTGGA
mIL-10	GCTCTTACTGACTGGCATGAG	CGCAGCTCTAGGAGCATGTG
mIL-6	ACAAAGCCAGAGTCCTTCAGAGAG	TTGGATGGTCTTGGTCCTTAGCCA
mIL-1β	TCTTTGAAGTTGACGGACCC	TGAGTGATACTGCCTGCCTG
mGAPDH	AGGTCGGTGTGAACGGATTTG	TGTAGACCATGTAGTTGAGGTCA
hArg-1	TTGGCTTGAGAGACGTGGAC	ACACTTGCTTCTCTATTACCTCAGA
hiNOS	ATGGAACATCCCAAATACGA	GTCGTAGAGGACCACTTTGT
hIL-10	ACCACGCTTTCTAGCTGTTGA	GCTCCCTGGTTTCTCTTCCTA
hIL-6	TGCCTCTTTGCTGCTTTCACA	TCGGTCCAGTTGCCTTCTCCC
hIL-1β	GGATATGGAGCAACAAGTGG	ATGTACCAGTTGGGGAACTG
hGAPDH	GGACCTGACCTGCCGTCTAG	GTAGCCCAGGATGCCCTTGA

Table S1: Primers used in Real-time quantitative PCR analyses. Related to Figures 5, 6, S5, and S6.